

MEASUREMENT NOISE IN PHOTOMETRIC STEREO BASED SURFACE RECONSTRUCTION

Toni Kuparinen, Ville Kyrki

Department of Information Technology, Lappeenranta University of Technology, P.O. Box 20, 53851 Lappeenranta, Finland

Pekka Toivanen

Department of Computer Science, University of Kuopio, P.O.Box 1627, 70211 Kuopio, Finland

Keywords: Surface reconstruction, photometric stereo, gradient fields, Fourier domain, Wiener filter, denoising, white noise.

Abstract: In this paper, we present a noise reduction method for photometric stereo based surface reconstruction of surfaces with high frequency height variation. Such surfaces are important for many industrial settings, for example, in paper and textile manufacturing. The paper presents the derivation of the effect of white image noise to gradient fields. Based on the derivation, a denoising approach of the gradient fields using the Wiener filter is proposed. Several known surface reconstruction methods with and without the proposed denoising approach are evaluated experimentally, with respect to the effect of the noise, and the boundary conditions of the reconstruction. The experimental results validate that the proposed approach improves the surface reconstruction on surfaces with high frequency height variation.

1 INTRODUCTION

Surface topography is a highly important quality parameter in many industrial applications, such as paper and textile manufacturing. Undesired surface topography variations can reflect imperfections in manufacturing process, product operational efficiency, and life expectancy. Depth recovery techniques, such as shape from shading (SfS) (Horn, 1990), and photometric stereo (PS) (Woodham, 1978), can provide surface gradients in a fast and non-contact manner. In order to obtain the surface topography, that is, the relative height values of the surface, the differential surface gradients have to be integrated. However, in practice the surface gradients are corrupted by noise, resulting from imaging and other measurement errors.

Several solutions have been proposed to integrate the measured gradient fields. A traditional method for integrating the surface height from gradient information is the Frankot-Chellappa algorithm (Frankot and Chellappa, 1988). Another popular method is the Poisson solver (Simchony et al., 1990). Typically, the performance of the surface reconstruction methods has been evaluated on surfaces with large, smooth objects, such as flower pots, faces, peaks, and ramps with rather strong additive Gaussian noise (Noakes

and Kozera, 2003; Karacali and Snyder, 2004; Wei and Klette, 2003; Agrawal et al., 2006).

However, monitoring of surface roughness and texture, that is, higher frequency variations with limited noise levels, are frequently of interest in manufacturing processes. McGunnigle (McGunnigle and Chantler, 2003) presented a framework for measurement and modelling of rough surfaces. They evaluated several surface description models, but did not reconstruct surfaces with or without noise. Recently Hansson (Hansson and Johansson, 2000) has studied two-light photometric stereo in paper surface reconstruction. Based on Hansson's work, Kuparinen extended the Hansson's two light method to four-light photometric stereo using Symmetrical binary weights in (Kuparinen et al., 2007). Kuparinen also showed that the minimization based Frankot-Chellappa and Poisson methods smooth the reconstructed surface removing the inherent high-frequency containing signal (Kuparinen et al., 2007).

This paper studies the photometric surface reconstruction of high-frequency varying surfaces. As particular contributions of the paper, a model of noise for the gradient images is derived, and an evaluation of the noise on reconstructed surfaces is presented. In addition, a denoising method based on Wiener filter-

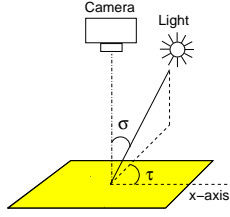


Figure 1: Geometry of the imaging setup. (Kuparinen et al., 2007)

ing is presented and evaluated on both artificial and real data. Drbohlav (Drbohlav and Chantler, 2005) derived also models for additive noise in photometric stereo, but did not present experimental results on noise reduction. Finally, the effect of the boundary conditions of the reconstruction is studied.

2 PHOTOMETRIC STEREO

2.1 The Estimation of Gradient Field

In photometric stereo, the viewing direction is held constant while the direction of the illumination between successive images is varied. Image radiance values in successive views are used to determine the surface orientation at each image point (Woodham, 1978). For Lambertian surfaces, the reflected intensity is independent of the viewing direction. However, the intensity depends on the direction of the light source.

Lambert's Law (Lambert, 2001) represents the image intensity i at the point (x, y)

$$i = \rho \lambda (\mathbf{I}^T \cdot \mathbf{n}), \quad (1)$$

where ρ is the surface albedo, λ is the intensity of the light source, $\mathbf{n} = [n_1, n_2, n_3]^T = \frac{[p, q, 1]^T}{\sqrt{p^2 + q^2 + 1}}$ is the unit normal to the surface and $\mathbf{I} = [\cos(\tau)\sin(\sigma), \sin(\tau)\sin(\sigma), \cos(\sigma)]^T$ is the unit vector toward the light source. Elements p and q are surface partial derivatives measured along the x and y axes, respectively. The angles of illumination, the tilt τ , and slant σ are illustrated in Fig. 1. Orthogonal projection and constant illumination over the surface are assumed in Lambert's Law.

For a four-light case, if the same slant angle σ is used for all light sources, and the tilt angles 0° , 180° , 90° and 270° are used for images i_1 through i_4 , respectively, the surface gradient fields can be derived using photometric stereo as follows:

$$p = \frac{2}{\tan(\sigma)} \frac{i_1 - i_2}{(i_1 + i_2 + i_3 + i_4)} \quad (2)$$

and

$$q = \frac{2}{\tan(\sigma)} \frac{i_3 - i_4}{(i_1 + i_2 + i_3 + i_4)}, \quad (3)$$

where i_1 and i_2 are intensity vectors of 0° and 180° tilt angles, and i_3 and i_4 intensity vectors of 90° and 270° tilt angles.

2.2 Reconstruction Methods

In order to obtain surface topography, the surface gradients have to be integrated. However, in practice the surface gradients contain noise, which can be derived from imaging and other measurement errors.

If the gradient fields are samples from a larger surface, e.g., textile or paper surface, the boundary conditions of the gradient fields are of high importance. Traditionally, the boundary conditions are omitted, since the object to be reconstructed is extracted from its surroundings, i.e., the edges of images are black, and the boundary conditions are not then relevant.

In surface reconstruction, one of three different boundary conditions is usually applied: Dirichlet, Neumann, or periodic boundary condition. Dirichlet boundary condition assumes that the height values of the boundary are known. Usually, this accounts to setting the height values at the boundary to zero. Neumann boundary conditions assume that the directed derivatives of the boundary are known, usually that the directed gradients of the boundary can be set to zero. In periodic boundary conditions, the surface is assumed to continue periodically, i.e., the surface continues identically to the other side, similar to the discrete Fourier transform (Simchony et al., 1990).

Next, particular solutions to the problem of integrating the measured gradient fields are described and then subsequently experimentally evaluated in the next section.

Hansson and Johansson presented a two-light PS method in (Hansson and Johansson, 2000). The imaging was modeled as

$$s'_p(x, y) = s_p(x, y) * PSF + n(x, y), \quad (4)$$

where $s_p(x, y)$ is the directional derivative, $n(x, y)$ is the noise, and $s_p(x, y) * PSF$ represents convolution of the signal by a point-spread function. They used a Wiener filter for the computation of the surface height from the directed derivatives. Boundary conditions in Hansson method are twofold: in gradient field estimation of p -gradient, the sum of height values are assumed to be zero, whereas in the integration phase, the periodic boundary conditions are used as the discrete Fourier transform is used. Thus, it is important to note that the method is not isotropic.

In Symmetric, similar assumptions for boundary conditions hold as for Hansson's method.

The Frankot-Chellappa (Frankot and Chellappa, 1988) algorithm aims to minimize the least square reconstruction error given by

$$J(Z) = \int \int ((Z_x - p)^2 + (Z_y - q)^2) dx dy, \quad (5)$$

where Z is the surface to be obtained, $\{Z_x, Z_y\}$ the gradient field of Z , and $\{p, q\}$ the given non-integrable gradient field. The gradient field of Z can be written as $\{Z_x, Z_y\} = \{p, q\} + \{\epsilon_x, \epsilon_y\}$, where $\{\epsilon_x, \epsilon_y\}$ denotes the correction gradient field, which makes the non-integrable field integrable (Agrawal et al., 2006). In Frankot-Chellappa method, periodic boundary conditions are applied, and the non-integrable gradient field is projected on to a set of integrable functions using the Fourier basis functions.

Simchony presented Poisson solver for surface reconstruction in (Simchony et al., 1990). The approach is similar to Frankot-Chellappa, such that the norm of the correction gradient field, Equation 5, is minimized. The second partial derivatives in Poisson equation are approximated using central differencing method. Simchony (Simchony et al., 1990) develops two algorithms for Poisson solver: 1) finite difference calculation in Fourier domain with periodic boundary conditions, and 2) finite difference calculation in time domain with Neumann boundary conditions.

2.3 Noise in Photometric Stereo

In practice, the surface gradients contain noise, which can be derived from imaging and other measurement errors. So far, the effect of the noise has not been thoroughly examined. If the imaging conditions are stable, the noise level of the sensors can be assumed stationary and measurable, and the information can be used in order to evaluate the effect of the noise on the gradient field and the final reconstructed surface.

Next, we propose a derivation for the influence of imaging noise to the gradient fields. We also propose a method for the restoration of the degraded gradient fields for photometric stereo. We make the assumption that additive white noise, $N(0, s^2)$, affects all the captured images: zero mean, Gaussian random variation with variance s^2 is added to images.

Taking into account the noise, Equation 2 can be written as

$$\begin{aligned} p &= \frac{2}{\tan(\sigma)} \frac{(i_1 + N_1(0, s^2)) - (i_2 + N_2(0, s^2))}{\sum_{k=1}^4 (i_k + N_k(0, s^2))} \\ &= \frac{2}{\tan(\sigma)} \frac{i_1 - i_2 + N(0, 2s^2)}{\sum_{k=1}^4 i_k + N(0, 4s^2)}. \end{aligned} \quad (6)$$

Note that the variance of the sum of two independent normal distributions is the sum of the distribution variances.

In the denominator of Equation 6, the effect of the noise can be excluded, when $\sum_{k=1}^4 i_k \gg 0$ and $N(0, 4s^2)$ is close to zero, that is, when the noise variance is small. This assumption is true for many industrial applications where the imaging conditions can be kept good and stable. Using the assumption and separating the gradient and the noise, the gradients are then

$$p = \frac{2}{\tan(\sigma)} \frac{i_1 - i_2}{(\sum_{k=1}^4 i_k)} + n, \quad (7)$$

and

$$q = \frac{2}{\tan(\sigma)} \frac{i_3 - i_4}{(\sum_{k=1}^4 i_k)} + n, \quad (8)$$

with the noise n for both gradient fields

$$n = \frac{2}{\tan(\sigma)} \frac{N(0, 2s^2)}{(\sum_{k=1}^4 i_k)}. \quad (9)$$

Making a further assumption that the noise variance is constant over the whole gradient image, the power spectrum of the noise field, $N(u, v)$, can be approximated as a constant field by averaging the sum of intensity images:

$$N(u, v) = \frac{2}{\tan(\sigma)} \frac{2s^2}{\frac{1}{MN} \sum_{x=1}^M \sum_{y=1}^N i_a(x, y)}, \quad (10)$$

where $i_a = \sum_{k=1}^4 i_k$, and the image size is $M \times N$ pixels. The effect of white noise can be derived in an identical manner for other combinations of slant and tilt angles for photometric stereo.

Wiener filtering is an optimal approach for restoring images degraded by noise, when the Signal-to-Noise Ratio (SNR) and Point Spread Function (PSF) are correctly known (Gonzalez and Woods, 2002). We propose that Wiener filtering is applied to gradient fields to restore them from the noise. In this work, PSF is omitted, and the Wiener filter is utilized in the Fourier domain as follows

$$H = \frac{1}{1 + SNR(u, v)^{-1}}, \quad (11)$$

where $SNR(u, v) = |G(u, v)|^2 / |N(u, v)|^2$ is the signal-to-noise ratio in the frequency domain. $G(u, v)$ is the power spectrum of the gradient field from photometric stereo, and $N(u, v)$ the power spectrum of the noise calculated using Equation 10.

3 EXPERIMENTS

Surface reconstruction methods Hansson, Symmetric, Frankot-Chellappa and Poisson solver are next evaluated on gradient fields of textured surfaces with high frequency variation and noise. The focus is to

evaluate the effect of noise level, denoising, and the boundary conditions for the integration methods in surface reconstruction. Evaluation measure is the surface reconstruction error. Two versions of the Poisson solver are evaluated: 1) finite difference calculation in time domain with Neumann boundary conditions, and 2) finite difference calculation in Fourier domain with periodic boundary conditions, denoted as Poisson, and Poissonf, respectively.

The evaluation is performed for both simulated data and real application data. Gradient fields are calculated using two approaches: 1) analytically for the simulated surface, and 2) applying photometric stereo to real image data from paper surface for the application. Both surfaces contain high-frequency variation.

3.1 Simulated Data

A chirp-surface contains periodic variation of increasing frequency with time, the amplitude of the surface remaining constant, as shown in Figure 2. In the experiments, the frequency was increased logarithmically given the following equation for the surface:

$$S = \sin\left(\frac{2\pi f_0}{\ln(k)}(k^t - 1)\right), \quad (12)$$

where f_0 is the frequency at $t = 0$, k is the rate of exponential increase in frequency, and t is the time. For a surface $S(x, y)$, time t was defined as $t = 0.5(x + y)$. The chirp-function was differentiated analytically in order to obtain the horizontal and vertical gradient fields, which were degraded with two levels of additive white noise: 5 dB, and 10 dB. The noise levels were then calculated using Equation 10 from the standard deviation of gradient fields. The degraded gradient fields were Wiener filtered, and surfaces were integrated from the degraded and Wiener filtered gradient fields.

Figure 2 and Table 1 present the reconstructed surfaces and the reconstruction errors. In Fig. 2, the effects of boundary conditions are visible. For methods applying periodic boundary conditions, that is, Hansson, Symmetric, Frankot-Chellappa, and Poissonf, periodic reconstruction errors near the surface boundaries are clearly observable. Poisson solver with Neumann boundary conditions reconstructs the boundaries without any noticeable error. For Hansson, also the horizontal surface reconstruction error deteriorates the reconstruction result.

The reconstruction errors in Table 1 were calculated from surfaces, which were scaled to the zero mean and unit variance. Reconstruction errors between the chirp-surface, and reconstructed surfaces were analyzed with two measures: 1) root

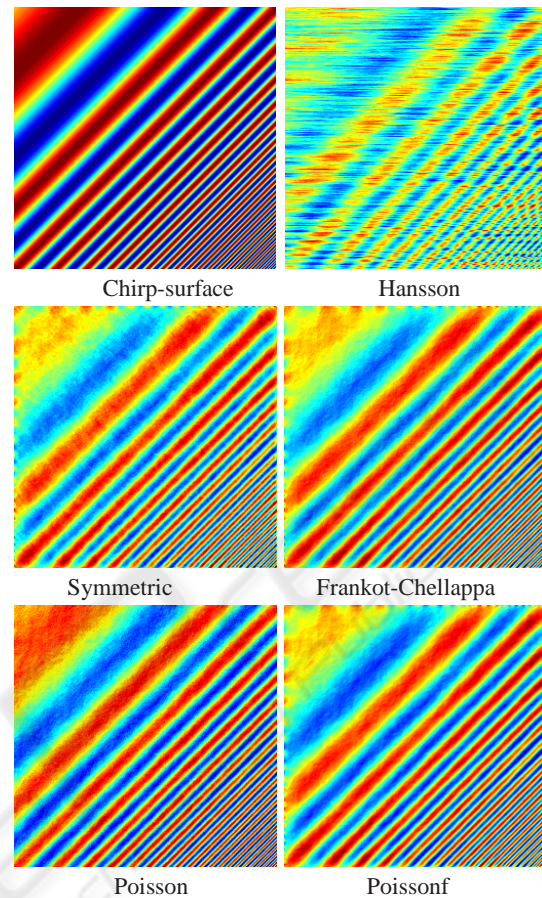


Figure 2: The original surface and the reconstructed surfaces from Wiener filtered gradient fields of simulation data.

mean square error (RMSE), and 2) high-pass RMSE (HPRMSE). The HPRMSE were calculated from surfaces, which were high-pass filtered with cutoff at 10% of resolution. RMSE emphasizes reconstruction errors on longer wavelengths, HPRMSE errors on higher frequencies.

In RMSE error, the Poisson solver with Neumann boundary conditions outperforms clearly the other methods in all the noise levels. At the same time, the reconstruction error in longer wavelengths for Hansson is significantly larger. Wiener filtering has only a minor effect to RMSE in surface reconstruction. In high-frequency reconstruction error, Poissonf outperforms the other methods, with Symmetric and Frankot-Chellappa being comparably close. Hansson and Poisson exhibit remarkably larger reconstruction errors in HPRMSE. It is also evident that the proposed Wiener filtering enhances the reconstruction results in high frequencies on 5 dB noise level.

Table 1: Surface reconstruction errors: RMSE, and High-pass RMSE calculated from 10% high pass filtered surfaces. S , S_n , and S_{wnr} are the reconstruction errors from original gradient fields, noise added gradient fields, and Wiener filtered gradient fields at 10 dB and 5 dB noise levels. The smallest reconstruction errors for each experiment are bolded.

Simulated data	RMSE					HPRMSE				
	S	S_n 10dB	S_{wnr} 10dB	S_n 5dB	S_{wnr} 5dB	S	S_n 10dB	S_{wnr} 10dB	S_n 5dB	S_{wnr} 5dB
Gradient field		0.140	0.140	0.417	0.409		0.134	0.134	0.395	0.388
Hansson	0.417	0.513	0.513	0.861	0.852	0.136	0.292	0.292	0.622	0.615
Symmetric	0.252	0.260	0.260	0.306	0.306	0.022	0.030	0.030	0.070	0.068
Frankot-Chellappa	0.239	0.246	0.246	0.288	0.288	0.020	0.027	0.027	0.061	0.060
Poisson	0.161	0.168	0.168	0.223	0.223	0.095	0.097	0.097	0.119	0.118
Poissonf	0.239	0.245	0.245	0.286	0.285	0.013	0.019	0.019	0.048	0.047
Application data										
Gradient field		0.003	0.003	0.010	0.008		0.003	0.003	0.009	0.007
Hansson		0.035	0.035	0.108	0.105		0.023	0.023	0.073	0.069
Symmetric		0.034	0.034	0.106	0.101		0.028	0.028	0.089	0.082
Frankot-Chellappa		0.013	0.013	0.043	0.042		0.006	0.006	0.020	0.018
Poisson		0.014	0.014	0.044	0.042		0.007	0.007	0.022	0.019
Poissonf		0.013	0.013	0.041	0.040		0.005	0.005	0.016	0.015

3.2 Application Example

In the second experiment, paper surfaces were reconstructed from gradient fields calculated using photometric stereo. The OTF and SNR functions for Hansson, and Symmetric methods were as Hansson proposed in (Hansson and Johansson, 2000). The paper surface images for photometric stereo were acquired using a CCD camera with a resolution of 2048 x 2048 pixels with 12 bits per pixel. In the experiments, the image area was 15 mm x 15 mm.

Because no ground truth of the surface topology was available, the influence of white noise in surface reconstruction was studied using artificial noise, in a similar fashion to the simulated data. The reconstruction results from the two noise degraded gradient fields were contrasted to original reconstructed surfaces without added noise. Similar to previous experiment, Gaussian white noise was added to images, and the gradient fields were calculated from the degraded images by photometric stereo. Standard deviations of gray-scale values of images were applied in determination of the 5 dB and 10 dB noise levels. In the gradient field restoration with Wiener filter, the white noise field was determined using Equation 10.

The reconstruction results are presented in Fig. 3, and Table 1. In Fig. 3, the smoothing effect of minimization based Frankot-Chellappa and Poisson solvers can be observed. Hansson and Symmetrical sharpen the reconstruction result by Wiener filtering, which includes SNR and a PSF optimized for paper surfaces. The reconstruction errors due to noise are remarkably smaller for minimization based methods, than for Hansson and Symmetric, see Table 1. Wiener filtering of gradient fields can be seen to enhance the reconstruction results in 5 dB noise level. The effects

of boundary conditions are not clearly visible on this application data.

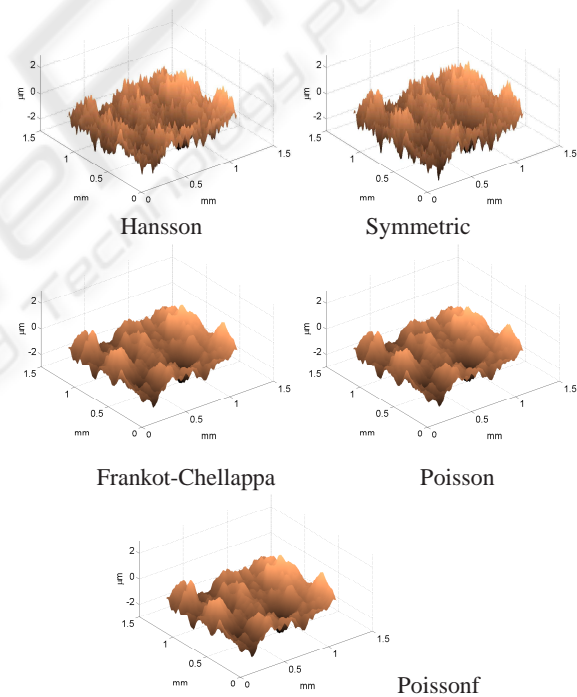


Figure 3: A fragment of reconstructed paper surfaces from Wiener filtered gradient fields.

For all the methods, the reconstruction errors increased with the noise level with simulated and real application data. In 10 dB noise level, the reconstruction results did not differ remarkably from the noiseless surfaces. Wiener filtering was able to denoise the gradient fields at 5 dB noise level. In RMS error, the Wiener filtering could not provide significant improvement in reconstruction result. However, the

high-pass reconstruction error was decreased 1%–2% with simulated data, and 5%–11% with real application data depending on the reconstruction method. In general, Wiener filtering improved the reconstruction result for all the methods and data sets.

4 CONCLUSIONS

In this paper, surface reconstruction techniques were studied in the context of surfaces with high frequency variation. The effect of imaging noise to gradient fields was also evaluated and a denoising approach was proposed.

The experiments demonstrated that the Wiener filtering based denoising of the gradient fields is useful and applicable, if the power spectrum of the noise is known. Minimization based surface reconstruction techniques, such as Poisson solver and Frankot-Chellappa, are more robust against the noise with simulated and real application data compared to Hansson and Symmetric, which perform the integration in Fourier domain with Wiener filtering. Hansson's method applies only one gradient field and was found to be more sensitive to correct Wiener filter parameters than Symmetric using two gradient fields. Poisson solvers with Neumann and periodic boundary conditions provided the best results in total and high frequency scale reconstruction, respectively. Neumann boundary conditions provided correct surface boundaries, whereas periodic boundary conditions deteriorated the surface boundary with a non-periodic pattern.

High frequency surfaces reconstructed using minimization based methods are still not adequate for some real applications, as they smoothen the surface making, for example, roughness measurements invalid. Frankot-Chellappa and Poisson solvers provide a robust and parameter free surface reconstruction in many cases, but the methods have to be developed further for high frequency containing data. Recent developments in surface reconstruction, such as α surfaces, M-estimators, regularization and diffusion, seem not to provide improvement for these problems, as their main effect is additional adaptive smoothing of the surface, as noted in (Agrawal et al., 2006). Thus, one problem in the reconstruction of high frequency surfaces is in the definition of the function to be minimized. In future work, minimization constraints for the surface reconstruction methods need to be studied. Another approach would be to model the imaging system more accurately, for example, using Wiener filtering with SNR and PSF. In this work, only the effect of the SNR was evaluated, and in future works also the

PSF has to be studied.

ACKNOWLEDGEMENTS

The authors gratefully appreciate the provided funding from European Regional Development Fund (ERDF), Finnish Funding Agency for Technology and Innovation (TEKES), Stora Enso, UPM, Metso, and Future Printing Center (FPC).

REFERENCES

- Agrawal, A., Raskar, R., and Chellappa, R. (2006). What is the range of surface reconstructions from a gradient field? In *Proc. ECCV*, pages 578–591.
- Drbohlav, O. and Chantler, M. (2005). On optimal light configurations in photometric stereo. In *Proc. IEEE ICCV*.
- Frankot, R. and Chellappa, R. (1988). A method for enforcing integrability in shape from shading algorithms. *IEEE PAMI*, 10(4):435–446.
- Gonzalez, R. and Woods, R. (2002). *Digital Image Processing*. Prentice Hall.
- Hansson, P. and Johansson, P.-A. (2000). Topography and reflectance analysis of paper surfaces using a photometric stereo method. *Opt. Eng.*, 39(9):2555–2561.
- Horn, B. (1990). Height and gradient from shading. *Int. J. Comput. Vision*, 5(1):37–75.
- Karacali, B. and Snyder, W. (2004). Noise reduction in surface reconstruction from a given gradient field. *International Journal of Computer Vision*, 60:25–44.
- Kuparinen, T., Kyrki, V., Mielikainen, J., and Toivanen, P. (2007). On surface reconstruction from gradient fields. In *Proc. of IEEE ICIP*, pages II 545–548.
- Lambert, J. (2001). *Photometry, or, on the measure and gradations of light, colors, and shade: translation from the Latin of photometria, sive, de mensura et gradibus luminis, colorum et umbrarum*. Illuminating Engineering Society of North America.
- McGunnigle, G. and Chantler, M. (2003). Rough surface description using photometric stereo. *Measurement Science and Technology*, 14:699–709.
- Noakes, L. and Kozera, R. (2003). Nonlinearities and noise reduction in 3-source photometric stereo. *Journal of Mathematical Imaging and Vision*, 18:119–127.
- Simchony, T., Chellappa, R., and Shao, M. (1990). Direct analytical methods for solving Poisson equations in computer vision problems. *IEEE PAMI*, 12(5):435–446.
- Wei, T. and Klette, R. (2003). Depth recovery from noisy gradient vector fields using regularization. In *Proc. of CAIP*, pages 116–123.
- Woodham, R. (1978). Photometric stereo. MIT A.I. Laboratory Memo. No. 479.